IL NUOVO CIMENTO **44 C** (2021) 176
DOI 10.1393/ncc/i2021-21176-4

Colloquia: La Thuile 2021

Rare decays from NA62

V. Duk(*)
INFN, Sezione di Perugia - Perugia, Italy

received 16 September 2021

Summary. — Recent results from the NA62 experiment at CERN are presented. The analysis of the $K^+ \to \pi^+\nu\bar{\nu}$ decay has been performed with the full dataset available. Upper limits have been set on the BR($\pi^0 \to$ *invisible*) and BR($K^+ \to \pi^+ X$) where X is a new scalar or pseudoscalar particle. The preliminary result on the formfactor measurement in the decay $K^+ \to \pi^+\mu^+\mu^-$ is reported.

(*) For the NA62 Collaboration: R. Aliberti, F. Ambrosino, R. Ammendola, B. Angelucci, A. Antonelli, G. Anzivino, R. Arcidiacono, T. Bache, A. Baeva, D. Baigarashev, M. Barbanera, J. Bernhard, A. Biagioni, L. Bician, C. Biino, A. Bizzeti, T. Blazek, B. Bloch-Devaux, V. Bonaiuto, M. Boretto, M. Bragadireanu, D. Britton, F. Brizioli, M.B. Brunetti, D. Bryman, F. Bucci, T. Capussela, J. Carmignani, A. Ceccucci, P. Cenci, V. Cerny, C. Cerri, B. Checcucci, A. Conovaloff, P. Cooper, E. Cortina Gil, M. Corvino, F. Costantini, A. Cotta Ramusino, D. Coward, G. D'Agostini, J. Dainton, P. Dalpiaz, H. Danielsson, N. De Simone, D. Di Filippo, L. Di Lella, N. Doble, B. Dobrich, F. Duval, V. Duk, D. Emelyanov, J. Engelfried, T. Enik, N. Estrada-Tristan, V. Falaleev, R. Fantechi, V. Fascianelli, L. Federici, S. Fedotov, A. Filippi, M. Fiorini, J. Fry, J. Fu, A. Fucci, L. Fulton, E. Gamberini, L. Gatignon, G. Georgiev, S. Ghinescu, A. Gianoli, M. Giorgi, S. Giudici, F. Gonnella, E. Goudzovski, C. Graham, R. Guida, E. Gushchin, F. Hahn, H. Heath, J. Henshaw, E.B. Holzer, T. Husek, O. Hutanu, D. Hutchcroft, L. Iacobuzio, E. Iacopini, E. Imbergamo, B. Jenninger, J. Jerhot, R.W. Jones, K. Kampf, V. Kekelidze, S. Kholodenko, G. Khoriauli, A. Khotyantsev, A. Kleimenova, A. Korotkova, M. Koval, V. Kozhuharov, Z. Kucerova, Y. Kudenko, J. Kunze, V. Kurochka, V. Kurshetsov, G. Lanfranchi, G. Lamanna, E. Lari, G. Latino, P. Laycock, C. Lazzeroni, M. Lenti, G. Lehmann Miotto, E. Leonardi, P. Lichard, L. Litov, R. Lollini, D. Lomidze, A. Lonardo, P. Lubrano, M. Lupi, N. Lurkin, D. Madigozhin, I. Mannelli, A. Mapelli, F. Marchetto, R. Marchevski, S. Martellotti, P. Massarotti, K. Massri, E. Maurice, M. Medvedeva, A. Mefodev, E. Menichetti, E. Migliore, E. Minucci, M. Mirra, M. Misheva, N. Molokanova, M. Moulson, S. Movchan, M. Napolitano, I. Neri, F. Newson, A. Norton, M. Noy, T. Numao, V. Obraztsov, A. Ostankov, S. Padolski, R. Page, V. Palladino, A. Parenti, C. Parkinson, E. Pedreschi, M. Pepe, M. Perrin-Terrin, L. Peruzzo, P. Petrov, Y. Petrov, F. Petrucci, R. Piandani, M. Piccini, J. Pinzino, I. Polenkevich, L. Pontisso, Yu. Potrebenikov, D. Protopopescu, M. Raggi, A. Romano, P. Rubin, G. Ruggiero, V. Ryjov, A. Salamon, C. Santoni, G. Saracino, F. Sargeni, S. Schuchmann, V. Semenov, A. Sergi, A. Shaikhiev, S. Shkarovskiy, D. Soldi, V. Sugonyaev, M. Sozzi, T. Spadaro, F. Spinella, A. Sturgess, J. Swallow, S. Trilov, P. Valente, B. Velghe, S. Venditti, P. Vicini, R. Volpe, M. Vormstein, H. Wahl, R. Wanke, B. Wrona, O. Yushchenko, M. Zamkovsky, A. Zinchenko.

1. – Introduction

The main goal of the NA62 experiment is the measurement of the branching ratio (BR) of the ultrarare decay $K^+ \to \pi^+\nu\bar{\nu}$. This flavour changing neutral current process (FCNC) can be described by the box and penguin diagrams. The BR value is very small due to the strong Cabibbo suppression and the quadratic GIM mechanism. The short-distance top quark loop is dominant in the decay amplitude, with a non-negligible contribution from the charm quark loop. The hadronic matrix element relevant for the $K \to \pi$ transition can be extracted from the $K^+ \to \pi^0 e^+ \nu_e$ decay taking into account the isospin correction. The BR value predicted by the Standard Model (SM), with CKM matrix elements from tree-level processes, has the precision O(10%): BR($K^+ \to \pi^+\nu\bar{\nu}$, SM) = $(8.4 \pm 1.0)\times10^{-11}$ [1, 2]. The main uncertainty comes from the external inputs. Due to the low uncertainty of BR(SM), the decay is sensitive to physics beyond the SM [3-8].

The byproducts of the analysis of the $K^+ \to \pi^+\nu\bar{\nu}$ decay are the search for a new particle in the $K^+ \to \pi^+ X$ decay and the study of the $\pi^0 \to$ *invisible* process if π^0 is tagged from the $K^+ \to \pi^+\pi^0$ decay. Beyond the baseline, the experiment allows to study rare kaon decays with 3 tracks in the final state, *e.g.* $K^+ \to \pi^+\mu^+\mu^-$ which allows to test the lepton flavor universality.

2. – NA62 experiment

The NA62 is a fixed target experiment located at the CERN SPS. Primary protons impinge on a beryllium target producing secondary particles. A 100 m long beam line collimates, focuses and transports charged particles of (75.0±0.8) GeV/c momentum to the decay volume. The kaon fraction in the secondary beam is 6%.

The setup is shown in fig. 1. Beam kaons are identified and timestamped by the KTAG, a differential Cherenkov detector filled with nitrogen and placed in the beam. The Gigatracker (GTK) detector, composed of three silicon pixel stations, timestamps beam particles of all types and measures their momentum. The CHANTI detector, located after the GTK, allows to veto hadronic beam-detector interactions in the last GTK station.

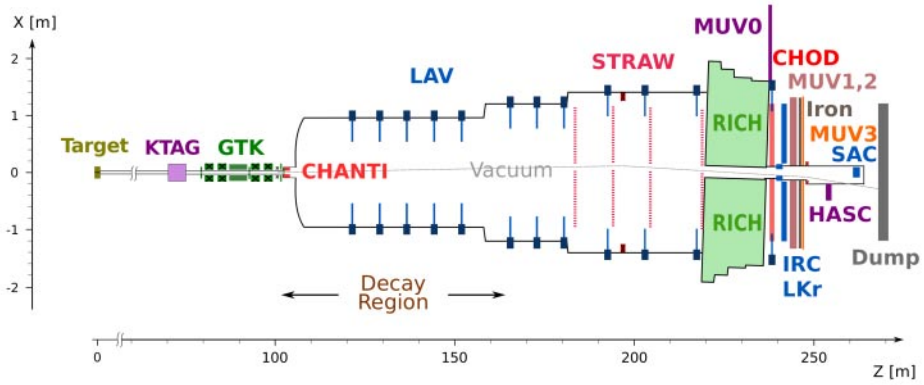

Fig. 1. – NA62 experimental setup.

The momentum of charged particles produced in kaon decays is measured by the magnetic spectrometer made of four straw chambers and a dipole magnet. A 17 m long RICH detector filled with neon at atmospheric pressure is used to identify π^+, μ^+, e^+ and together with a scintillator hodoscope (CHOD) measures the downstream time. Hadronic calorimeters (MUV1 and MUV2) and a fast scintillator muon veto (MUV3) are aimed at separating π^+ and μ^+. A system of photon veto detectors is implemented (12 LAV stations, LKr, IRC, SAC) in order to reject extra electromagnetic activity, covering angles up to 50 mrad. The detailed description of the setup can be found in [9].

3. – The $K^+ \to \pi^+\nu\bar{\nu}$ analysis

The main kinematic variable used in the analysis is the missing mass squared: $m^2_{miss} = (P_K - P_\pi)^2$. Here P_K and P_π are kaon and pion 4-momenta. The K^+ track is reconstructed and timestamped in the GTK. The intersection point of the GTK and STRAW tracks gives a kaon decay vertex which is required to be located within a 50 m fiducial region beginning 10 m downstream of the last GTK station. The downstream track is identified with two independent methods: a multivariate analysis with Boosted Decision Trees (BDT) using energy deposition, energy sharing and shower shape profiles in the electromagnetic (LKr) and hadronic calorimeters (MUV1/2), as well as signals from the muon veto (MUV3); a cut-based approach using the particle mass reconstructed by the RICH detector and a track-driven likelihood discriminant for the $\pi^+/\mu^+/e^+$ separation. Additionally a photon and multi-charged particle rejection is applied based on the information in the photon veto detectors and the CHOD. Two signal regions are defined: Region 1 (R1) in a (15–35) GeV/c momentum range and m^2_{miss} between 0 and 0.01 GeV$^2/c^4$; Region 2 (R2) in a (15–45) GeV/c momentum range and m^2_{miss} between 0.026 and 0.068 GeV$^2/c^4$. R1 and R2 are kept blind until the completion of the analysis. The decay $K^+ \to \pi + \pi^0$ is used for the normalization, since it allows to cancel systematic uncertainties due to K^+ and π^+.

The analysis of the 2016 and 2017 data sets are published [10, 11]. The 2018 data sample is split into two periods S1 and S2, before and after the installation of a new collimator. They correspond to 20% and 80% of the full statistics, respectively. The major improvements are applied to the S2 subsample, while the S1 follows the analysis procedure described in [11] with small optimizations.

The S2 sample is divided into 6 categories defined by 5 GeV/c-wide momentum bins from 15 to 45 GeV/c. The event selection is optimized for each category in order to achieve optimal signal sensitivity. The S1 sample is treated as a single category integrated over momentum due to smaller statistics with respect to S2.

The Single Event Sensitivity (S.E.S.) for the complete 2018 sample, integrated over all categories, is $S.E.S. = (1.11 \pm 0.07) \times 10^{-11}$, assuming the SM value for the BR. This corresponds to the expected signal yield $N^{expected}_{\pi\nu\nu} = 7.58 \pm 0.40_{syst} \pm 0.75_{ext}$. The background contamination is $N_{bkg} = 5.28^{+0.99}_{-0.74}$ composed of K decays (1.98 ± 0.15 events) and upstream background ($3.30^{+0.98}_{-0.73}$ events). The background predictions are validated using dedicated control regions.

After unblinding, seventeen events were found: thirteen in R1 and four in R2. Combining all available data samples, NA62 has observed 20 candidate events in both signal regions. The 2016 and 2017 samples are added as two separate categories (see fig. 2 right), and the final value of BR is obtained from the maximum likelihood fit over all the categories. The resulting branching ratio is BR($K^+ \to \pi^+\nu\bar{\nu}$) = ($11.0\ ^{+4.0}_{-3.5}\ \pm\ 0.3$) $\times\ 10^{-11}$,

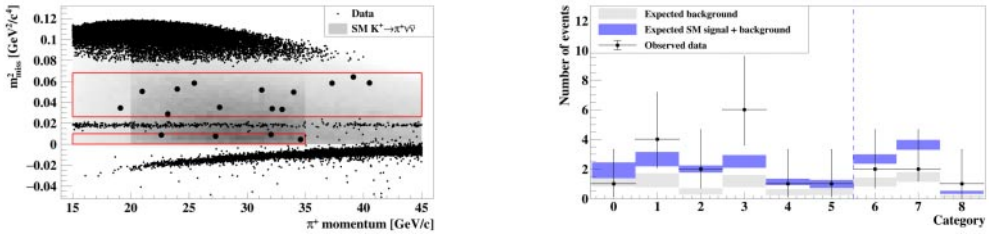

Fig. 2. – Left: reconstructed m^2_{miss} as a function of π^+ momentum satisfying the $K^+ \to \pi^+\nu\bar{\nu}$ selection criteria. The grey area corresponds to the expected distribution of $K^+ \to \pi^+\nu\bar{\nu}$ MC events. The two boxes define the signal regions R1 and R2. The events observed in R1 and R2 are shown together with the events found in the background and validation regions. Right: comparison between the expected and observed number of events for the categories used in the maximum likelihood fit to extract the $K^+ \to \pi^+\nu\bar{\nu}$ branching ratio. Categories 0 to 5 correspond to six 5 GeV/c-wide momentum bins of S2. Category 6, 7 and 8 correspond to S1, 2017 and 2016, respectively. The observed data for each category is indicated by the black dots. The grey boxes show the expected number of background events with the corresponding uncertainty. The blue shaded rectangles indicate the expected number of events summing the background contribution and a SM signal with its uncertainty.

which is compatible with the SM value within one standard deviation. The first uncertainty is statistical, dominated by the Poissonian fluctuation of the expected background, and the second one is systematic coming from the uncertainty of the signal expectation. The CLs method [12] is used to estimate the signal significance which is found to be 3.5 standard deviations. This is the most precise determination of the $BR(K^+ \to \pi^+\nu\bar{\nu})$ to date.

4. – Search for a new particle in the $K^+ \to \pi^+ X$ decay

Many extensions of the SM foresee the existence of a new feebly interacting scalar or pseudo-scalar particle X. If X lives long enough to decay outside the experimental apparatus, it can be searched for in the decay $K^+ \to \pi^+ X$ as a peak in the m^2_{miss} distribution. The search using the 2017 sample has been performed and published in [13]. The event selection and background sources are the same as for the $K^+ \to \pi^+\nu\bar{\nu}$ analysis, with the addition of the $K^+ \to \pi^+\nu\bar{\nu}$ itself which becomes the dominant background. No significant excess above the background is observed. To set the upper limits, each X-mass hypothesis is treated independently according to the CLs method. Upper limits for a stable or invisibly decaying particle are shown in fig. 3 left. For X decaying to SM particles the results are displayed in fig. 3 right for different values of τ_X. Previous limits from the E949 experiment [14] are improved for most mass hypotheses.

5. – Search for the $\pi^0 \to$ *invisible* decay

The search for the $\pi^0 \to$ *invisible* decay is a test of new physics involving feebly interacting particles. Any observation of this decay would be an indication of the physics beyond the SM. The search has been performed with the 2017 data sample using the π^0's produced in the $K^+ \to \pi^+\pi^0(\gamma)$ decay [15]. Such tagging allows to interprete the analysis results as a search for a new particle X (scalar or pseudoscalar) produced in

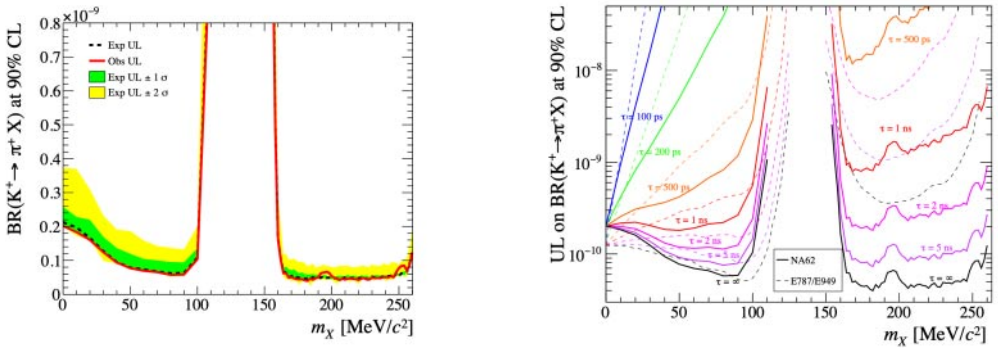

Fig. 3. – Left: upper limits on $BR(K^+ \to \pi^+ X)$ for each mass hypothesis, m_X, tested. Right: model-independent observed upper limits as functions of the mass and lifetime assumed for X for NA62 (solid lines) and E787/E949 (dashed lines).

the $K^+ \to \pi^+ X$ decay in the kinematic region not covered by the analysis described in sect. **4**.

The event selection includes the criteria used for the $K^+ \to \pi^+ \nu\bar{\nu}$ analysis and additional conditions to reject events from the $\pi^0 \to \gamma\gamma$ decay. The signal selection achieves a rejection power of $O(10^8)$ against $K^+ \to \pi^+\pi^0(\gamma)$. In the pion momentum range 25–40 GeV/c, 4.4×10^9 π^0 mesons are tagged. The expected background is $N_{bkg} = 10^{+22}_{-8}$. Twelve events consistent with $\pi^0 \to invisible$ are observed which is compatible with the background prediction. The upper limit is set on the number of signal events using the CLs method ($N_s < 8.24$) which is translated to the upper limit on the BR: $BR(\pi^0 \to invisible) < 4.4 \times 10^{-9}$ (90% CL). The results improves the previous limit by the factor of 60. The limits on the $BR(K^+ \to \pi^+ X)$ are shown in fig. 4 (X is a scalar particle) and fig. 5 (pseudoscalar).

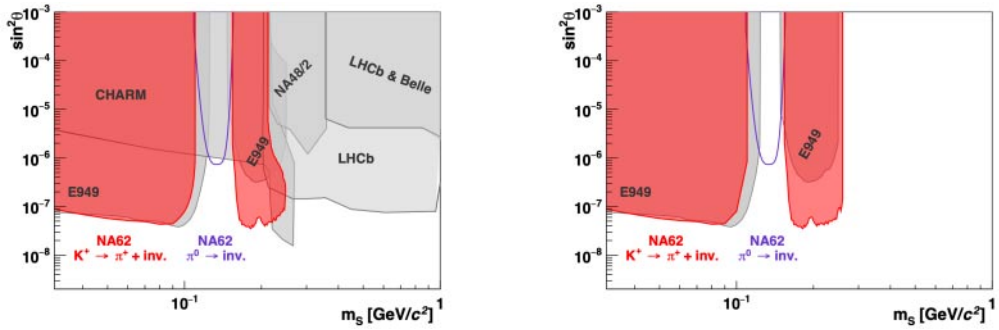

Fig. 4. – Excluded regions of the parameter space $(m_S, \sin^2\theta)$ for a dark scalar, S, of the BC4 model [16] decaying only (left) to visible SM particles as in the BC4 model and (right) invisibly. The exclusion bound from the search for the decay $K^+ \to \pi^+ S$ is labelled as $K^+ \to \pi^+ inv$ and is shaded in red. In the π^0 mass region the independent NA62 search for $\pi^0 \to invisible$ is shown in purple.

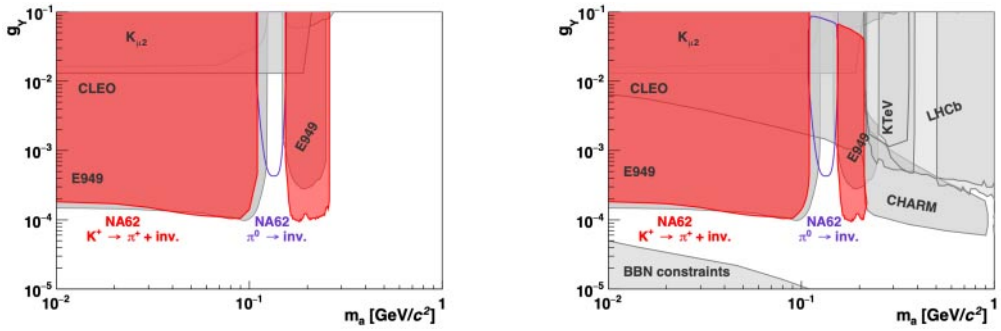

Fig. 5. – Excluded regions of the parameter space (m_a, g_Y) for an ALP, a, of the BC10 model [16] decaying only (left) to visible SM particles as in the BC10 model and (right) invisibly. The exclusion bound from the search for the decay $K^+ \to \pi^+ a$ is labelled as $K^+ \to \pi^+ inv$ and is shaded in red. In the π^0 mass region the independent NA62 search for $\pi^0 \to invisible$ is shown in purple.

6. – Study of the $K^+ \to \pi^+\mu^+\mu^-$ decay

The study of the FCNC decay $K^+ \to \pi^+\mu^+\mu^-$ is an important test of the lepton flavor universality (LFU). The differential width is expressed in terms of two Dalitz variables $z = [m(\mu^+\mu^-)/M_K]^2$ and $x = [m(\pi^+\mu^+)/M_K]^2$:

$$\frac{d^2\Gamma}{dzdx} = \frac{\alpha^2 M_K}{8\pi(4\pi)^4}[(2x + z - 2 - 2r_\mu^2)(-2x - z + 2r_\pi^2 + 2r_\mu^2) + z(z - 2 - 2r_\pi^2)]|W(z)|^2(1 + \delta(x, z))),$$

where $r_i = M_i/M_K$ [17,18] . The factor $1 + \delta(x, z)$ takes into account radiative effects, the formfactor $W(z)$ is introduced in the framework of the chiral perturbation theory:

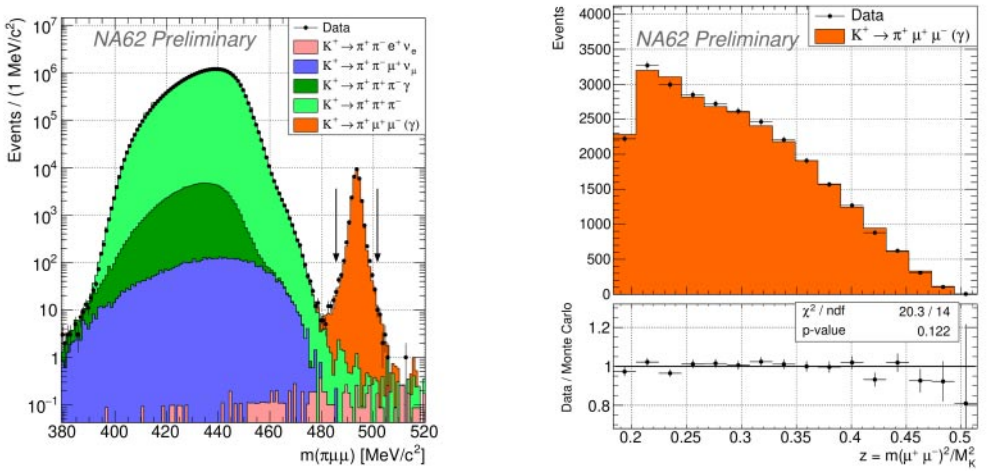

Fig. 6. – Left: reconstructed invariant mass $M(\pi\mu\mu)$. Right: z spectrum after the form factor fitting.

$W(z) = G_F M_K^2(a_+ + b_+ z) + W^{\pi\pi}(z)$, here $W^{\pi\pi}(z)$ is the contribution of three-pion decay term.

The analysis is based on the NA62 data collected in 2017 and 2018. For the normalization a topologically similar decay $K^+ \to \pi^+\pi^+\pi^-(K3\pi)$ is used. In total, 28011 signal candidates are selected with the background contamination (dominated by $K3\pi$) estimated to be $N_{bkg} = 12.5 \pm 1.7_{stat} \pm 12.5_{syst}$ events. The invariant mass $M(\pi\mu\mu)$ distribution is shown in fig. 6 left. The form factor parameters a_+ and b_+ are fitted using the reweighting of the MC z spectrum (fig. 6 right) and minimization of the $\chi^2(a_+, b_+)$ criterion quantifying the difference between the MC z spectrum corresponding to certain values of (a_+, b_+) and the experimental one. The best fit values are $a_+ = -0.592 \pm 0.015$ and $b_+ = -0.699 \pm 0.058$ which corresponds to the $BR = (9.27 \pm 0.11) \times 10^{-8}$. The obtained formfactor values are compatible with previous measurements in both muon and electron modes and thus no tension in LFU is observed. The NA62 result significantly improved the precision of the BR and formfactor measurements.

REFERENCES

[1] Buras A. J. *et al.*, *JHEP*, **11** (2015) 033.
[2] Brod J. *et al.*, *Phys. Rev. D*, **83** (2011) 034030.
[3] Blanke M. *et al.*, *JHEP*, **03** (2009) 108.
[4] Buras A. J. *et al.*, *JHEP*, **11** (2015) 166.
[5] Blazek T. and Matak P., *Int. J. Mod. Phys. A*, **29** (2014) 1450162.
[6] Isidori G. *et al.*, *JHEP*, **08** (2006) 064.
[7] Blanke M. *et al.*, *Eur. Phys. J. C*, **76** (2016) 182.
[8] Isidori *et al.*, *Eur. Phys. J. C*, **77** (2017) 618.
[9] The NA62 Collaboration, *JINST*, **12** (2017) P05025.
[10] The NA62 Collaboration, *Phys. Lett. B*, **791** (2019) 156.
[11] The NA62 Collaboration, *JHEP*, **11** (2020) 042.
[12] Read A. L., *J. Phys. G*, **28** (2002) 2693.
[13] Cortina Gil E. *et al.*, *JHEP*, **03** (2021) 058.
[14] Artamonov A. V. *et al.*, *Phys. Rev. D*, **79** (2009) 092004.
[15] The NA62 Collaboration, *JHEP*, **02** (2021) 201.
[16] Beacham J. *et al.*, *J. Phys. G*, **47** (2020) 010501.
[17] D'Ambrosio G. *et al.*, *JHEP*, **08** (1998) 004.
[18] Dubnickova A. *et al.*, *Phys. Part. Nucl. Lett.*, **5** (2008) 76.